Chemical Geology 388 (2014) 87–97

Contents lists available at ScienceDirect

Chemical Geology

journal homepage: www.elsevier.com/locate/chemgeo

YBCs sanidine: A new standard for $^{40}Ar/^{39}Ar$ dating

Fei Wang [a,*], Fred Jourdan [b], Ching-Hua Lo [c], Sebastien Nomade [d], Herve Guillou [d], Rixiang Zhu [a], Liekun Yang [a], Wenbei Shi [a], Huile Feng [a], Lin Wu [a], Haiqing Sang [a]

[a] State Key Laboratory of Lithospheric Evolution, Institute of Geology and Geophysics, Chinese Academy of Sciences, Beijing 100029, China
[b] JdL Centre & Department of Applied Geology Curtin University; GPO Box U1987, Perth, WA 6845, Australia
[c] Department of Geosciences, National Taiwan University, Taipei 106, Taiwan
[d] LSCE-Vallée Bât. 12, avenue de la Terrasse, F-91198 Gif-sur-Yvette Cedex, France

ARTICLE INFO

Article history:
Received 5 March 2014
Received in revised form 30 June 2014
Accepted 1 September 2014
Available online 16 September 2014

Editor: D.B. Dingwell

Keywords:
$^{40}Ar/^{39}Ar$ geochronology
New standard
YBCs sanidine

ABSTRACT

The $^{40}Ar/^{39}Ar$ dating technique is based on neutron fluence monitors (standards). Recent investigation demonstrates that currently used standards are not as homogenous as believed and new standards are needed (Philips and Matchan, 2013). In this study, we report a new sanidine standard, YBCs, collected from a phonolite at Yabachi in Tibet, China, for single-grain $^{40}Ar/^{39}Ar$ dating. Aliquots were distributed to four international laboratories for analysis and intercalibration.

The results show that YBCs crystals are homogenous in K content, $^{40}Ar^*/^{39}Ar_K$ (F-value) and age at the single grain level. The standard deviations of the F-value and age have small ranges from 0.29% to 0.53% and from 0.42% to 0.52%, respectively. These show that YBCs is a suitable standard for $^{40}Ar/^{39}Ar$ geochronology. The calibrated age of YBCs is 29.286 ± 0.206 Ma, or neglecting the error in the decay constant, 29.286 ± 0.045 Ma. Finally, the intercalibration factors (which allow direct comparison between standards) between YBCs and FCs, GA1550, ACs and HB3gr are calculated as: $R_{FCs}^{YBCs} = 1.044296 \pm 0.003968$, $R_{GA1550}^{YBCs} = 0.291261 \pm 0.001148$ $R_{ACs}^{YBCs} = 24.443066 \pm 0.068432$ and $R_{HB3gr}^{YBCs} = 0.020312 \pm 0.000885$. These values can be used to compare YBCs with other standards directly.

1. Introduction

The $^{40}Ar/^{39}Ar$ dating method is one of most widely applicable and precise methods of geochronology. It is based on the natural decay of ^{40}K to $^{40}Ar^*$ but since it is difficult to accurately measure the ratio of K (a solid) to Ar (a noble gas), the $^{40}Ar/^{39}Ar$ method is instead based on an indirect approach where a portion of the ^{39}K from the unknown sample is converted to ^{39}Ar by neutron activation (n, p reaction) in a nuclear reactor, as a proxy for ^{40}K. Therefore, a standard (crystals of a precisely known age) is needed to monitor the neutron flux (fluence). The fluence monitor is irradiated alongside the unknown samples. The "known" age of the standard or the fluence monitor is used to calculate the proportion of ^{39}K that has been converted to ^{39}Ar, which is in turn used to calculate the age of a sample (unknown) using the measured $^{40}Ar/^{39}Ar$ ratio. This makes the $^{40}Ar/^{39}Ar$ technique a relative dating technique, with the standard or the fluence monitor as the reference for the $^{40}Ar/^{39}Ar$ dating. Therefore, the absolute precision and accuracy of the $^{40}Ar/^{39}Ar$ method are directly dependent on the precision and accuracy on the age of the monitor used.

Although there are presently more than 15 standards used in $^{40}Ar/^{39}Ar$ geochronology (McDougall and Harrison, 1999), most of them have ages that have been demonstrated to be heterogenous at the single grain level and thus, not suitable for most modern $^{40}Ar/^{39}Ar$ applications (e.g. Jourdan and Renne, 2007, Heri et al., 2014). Currently, only handful standards are currently deemed suitable for $^{40}Ar/^{39}Ar$ geochronology (e.g. HB3gr, ACs, FCs, GA1550, TCs) (Renne et al., 1998; McDougall and Harrison, 1999; Nomade et al., 2005; Jourdan et al., 2006; Jourdan and Renne, 2007). Even then, when high-resolution step-heating measurements of these standards are carried out using the latest generation of multi-collection mass spectrometer, the tenfold more precise results show that even for standards such as FCs, the internal distribution of $^{40}Ar^*$ is heterogenous at the single grain level (Phillips and Matchan, 2013). Nevertheless, the total fusion age of FCs is fully reproducible at the grain to grain level, which is the most important quantity for a secondary $^{40}Ar/^{39}Ar$ standard. Therefore, testing a variety of intercalibrated standards is important, and in particular, blind calibration between several laboratories is highly desirable to cancel out any laboratory bias measurement that could arise from the calibration of a standard from a single noble gas instrument.

In this paper, we are reporting a new sanidine standard, YBCs. Blind calibration was carefully carried out between four laboratories, showing that it is homogenous in K content, $^{40}Ar^*/^{39}Ar_K$ (F-values) and age at the single grain level. Although more work is needed to reveal the "absolute" homogeneity of $^{40}Ar^*$ by using the latest generation of noble-gas spectrometers (e.g., ARGUS VI and Noblesse machine), the YBCs is the

* Corresponding author.
E-mail address: wangfei@mail.iggcas.ac.cn (F. Wang).

http://dx.doi.org/10.1016/j.chemgeo.2014.09.003
0009-2541/

first standard developed jointly in Australasia and Eurasia, and is more accessible to the Asian $^{40}Ar/^{39}Ar$ community. Furthermore, it is crucial for standards that will be distributed to the Asian community to be fully calibrated with well-known $^{40}Ar/^{39}Ar$ standards as this will allow direct comparison of any measured sample ages worldwide.

2. Geological setting

YBCs sanidine was collected from the Yabachi volcanic field located in central Tibet (Fig. 1). The Tibetan Plateau comprises the Songpan–Ganzi, Qiangtang and Lhasa Blocks from north to south (Yin and Harrison, 2000; Chung et al., 2005; Wang et al., 2010), which are separated by the Jinshajiang and Bangong sutures, respectively (Fig. 1). Eocene–Early Oligocene (50–29 Ma) volcanic and intrusive rocks are widespread in the Qiangtang Block (e.g., Chung et al., 2005; Spurlin et al., 2005; Jiang et al., 2006; Ding et al., 2007), due to an east-west extension and regional uplift of the Tibetan Plateau during that time (Wang et al., 2010).

The Yabachi volcanic field is located in the west of the Qiangtang Block, which is 5023 m above sea level (Fig. 1). The flat-topped Cenozoic volcanic rock hills are widely distributed in a 150 km^2 area overlying the Jurassic, Cretaceous and early Tertiary units (Fig. 2). Although the lavas were eroded into isolated hills by water runoff, three phrases of eruptions can still be recognized (Fig. 2). Petrologically, the volcanic rocks are alkaline, including aegirine-, riebeckite-, sodalite-, nosean-, hauyne-, leucite-, sanidine- and nepheline-bearing trachytes, phonolites, trachyandesites and pyroxenites (e.g. Ding et al., 2000; Wang et al., 2010). Located in the west of the Yabachi (Fig. 2), the Yulinshan volcanoes predominantly comprised phonolites and trachyandesites. The phonolite is characterized by large phenocrysts (2–10 mm) of sanidine residing in the cryptocrystalline groundmass (Fig. 3A). The sanidine samples studied in the present work were collected from the phonolite (Fig. 3B).

3. Geochemistry

3.1. Major elements of the phonolite

The abundance of major elements was determined by using X-ray fluorescence spectrometry (XRF) method with a Philips PW 1400 spectrometer at the IGGCAS (Institute of Geology and Geophysics, Chinese Academy of Sciences). Analytical uncertainties range from 2% to 5%.

The results of the major element analyses of the phonolite are shown in Table 1. The phonolite is relatively primitive with SiO_2 from 54.39 to 55.11%. It has high alkali contents (K_2O = 7.28–7.38% and Na_2O = 4.57–4.87%), and relatively high total Fe (Fe_2O_3 + FeO) (8.8%), medium CaO (4.04 wt.%), but low abundances in MnO (0.14–0.19%), TiO_2 (0.88–0.95%) and P_2O_5 (0.12–0.14%).

3.2. Electronic microprobe analyses of the YBCs sanidine

YBC sanidine grains were fixed to epoxy, polished and C-coated for electron microprobe (EMP) analysis at the IGGCAS. Electron microprobe analyses were performed on a JEOL JXA-8100 electron microprobe with a WDS/EDS combined micro-analyzer. The analytical conditions were as follows: 15 kV constant accelerating voltage, 20 nA beam current and 2 μm nominal beam diameter. The counting time varied between 10 s

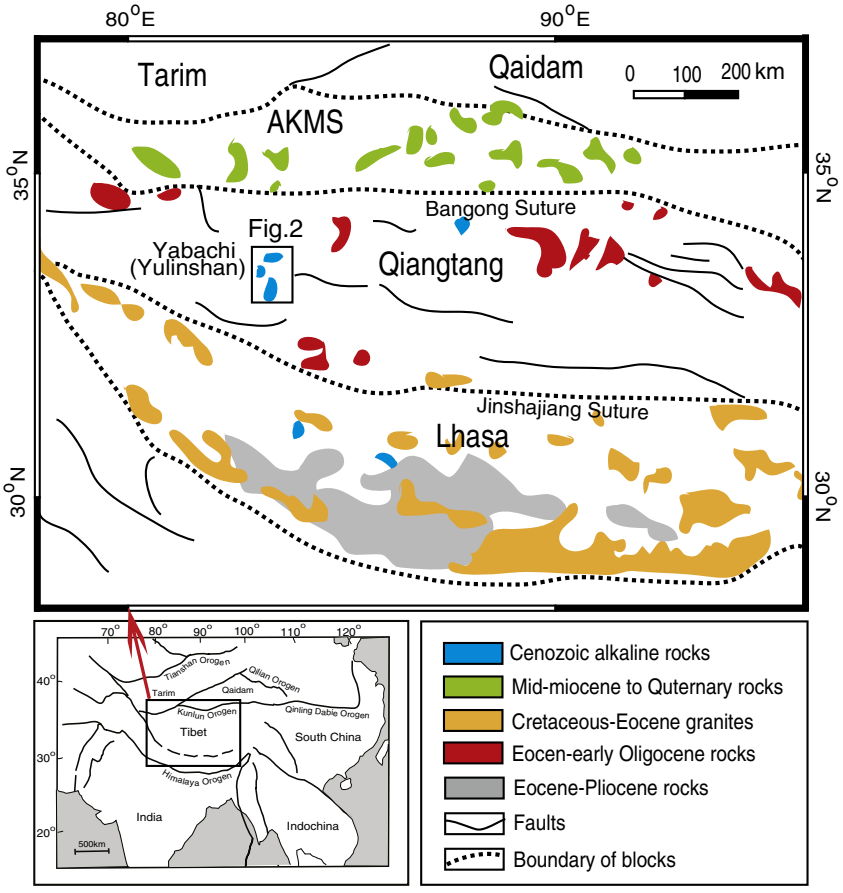

Fig. 1. Map of the Tibetan Plateau showing major crustal blocks and spatial distribution of Cenozoic volcanic rocks (modified from Yin and Harrison, 2000, and Chung et al., 2005). The inset shows a broader region with major tectonic framework.

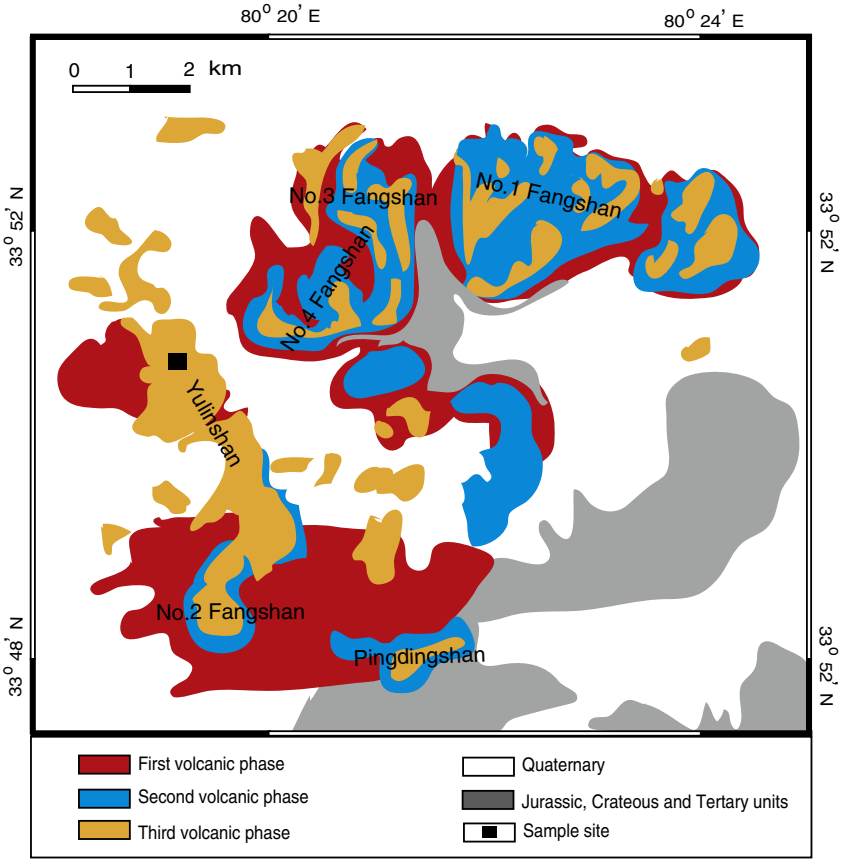

Fig. 2. Distribution map of the Yabachi volcanic field. The lavas of the three phases and other geological units are shown. The site of YBC sample is indicated (modified from Ding et al., 2000).

and 30 s for different elements. Natural and synthetic oxides were used as standards, and a computer program to implement the ZAF procedure was used for calibration. Repeated analyses of standards show a typical precision of ± 1% for major and ± 5% for minor elements. The back-scattered electron (BSE) images were also acquired on the same instrument.

The BSE image taken at the highest contrast settings shows that the YBCs are euhedral and pristine (Fig. 4A), implying that they were cooled rapidly and did not react with the matrix. EMP further data indicate that they are chemically homogenous at the single grain level (Fig. 4A and B). Some grains in the population showed scratches on the crystal surface due to the sample preparation (Fig. 4B and C). Overall, the in-situ electronic microprobe analyses indicate that the YBCs are chemically pure K-feldspar.

Fifteen grains of the YBCs sanidine were selected for EMP analysis. Data are shown in Appendix Table 1; the arithmetic means of the individual analyses are listed in Table 2. Sixteen to twenty-five points were analyzed on each grain (total 291 analyses, Fig. 5, Appendix Table 1). The majority of YBC sanidine grains display a high and consistent abundance of K_2O ranging from 11.47 to 12.50 wt.% with an arithmetic-mean and standard deviation of 12.23 ± 0.24 wt.% when the 16 outlier analyses are deleted (Fig. 5, Table 2 and Appendix Table 1). Due to the low CaO contents (0.05 to 0.17 wt.%) of the sanidine crystals close to background level, the K/Ca ratio, derived from $^{39}Ar/^{37}Ar$, varies from 80 to 220 and is therefore not a reliable indicator for the chemical composition (Fig. 5). During the microprobe analyses, neither inclusions nor compositional variation due to chemical zoning were observed in any of the sanidine crystals.

4. $^{40}Ar/^{39}Ar$ analyses of YBCs sanidine

4.1. Scheme and design

1500 kg fresh rock of YBC phonolite was collected and moved from Tibet to a commercial company in Langfang, Hebei province in China, for mineral separation. The rock was first disintegrated and crushed. After sieving, mineral grains and rock chips in the range 0.28–0.45 mm (60–40 mesh) were obtained. Without going through the usual mineral separation methods such as heavy liquids and Frantz magnetic separation, the grains and chips were handpicked directly under a binocular microscope to collect the sanidine crystals. Crystals with visible impurities and iron-mottling were removed. A total of 910 g of pure, fresh sanidine crystals were collected from the 1500 kg of rock. The grains were then cleaned ultrasonically twice in acetone and then in water, 20 min for each. After being fully mixed, the YBC sanidine crystals were divided into 90 bottles, 10 g in each.

Six aliquots (A-1 to A-6) of the YBCs crystals from the same bottle were dispatched to $^{40}Ar/^{39}Ar$ laboratories at the IGGCAS (China), National Taiwan University (Taiwan), Curtin University (Australia) and Gif-Sur-Yvette of CEA-CNRS UVSQ (France). Single grain laser-fusion analyses of YBCs were carried out relatively to five different standards (HB3gr, FCs, GA1550, TCs and ACs) by using different mass-spectrometers (MAP 215-50, VG5400 and VG3600). In addition, to assess the homogeneity of $^{40}Ar^*/^{39}Ar_K$, the step-heating technique was used on a bulk sample (3 mg, ~10 crystals) at IGGCAS.

The multi-laboratory approach allows us to test if there is any bias arising from the use of different batches of primary standards and

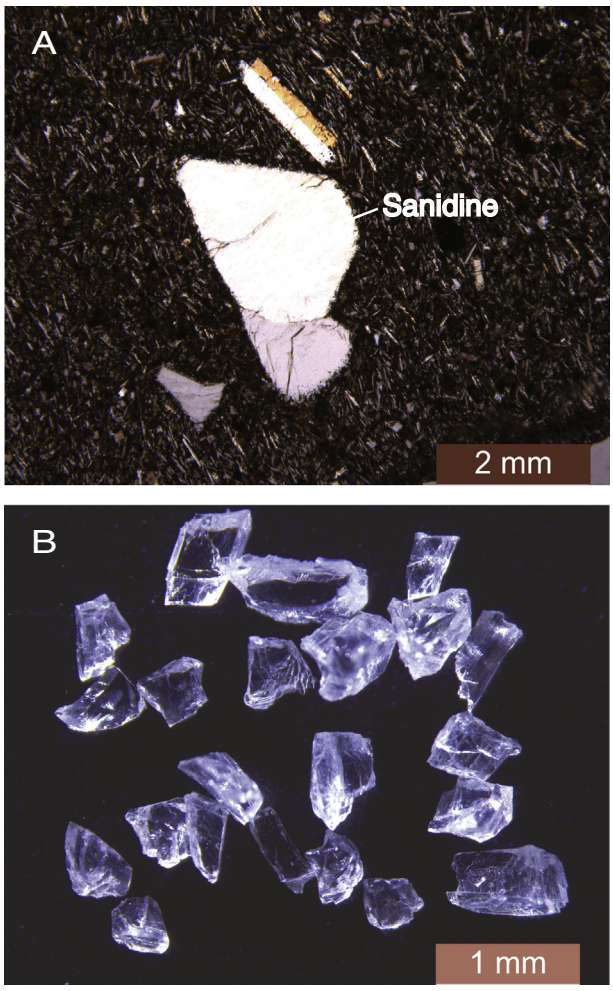

Fig. 3. A: Microphotograph of YBC phonolite showing regular sanidine phenocrysts crystals residing in the cryptocrystalline groundmass. B: Photo of YBC sanidine grains of clear and pure crystals.

machines and more importantly, to cancel out any minor inter-laboratory variations assuming that these are due to random chance (in other words, this allows smoothing the noise inherent to the technique). Ultimately, provided that the homogeneity of the YBCs standard can be demonstrated, this approach allows obtaining better precision on the age and $^{40}K/^{40}Ar^*$ value due to the increase of counting statistics.

4.2. Analytical procedure

An important set of values determined during this study are the R-values which allow the comparison of standards with each other and the $^{40}K/^{40}Ar^*$ value of YBCs; both being independent of the set of decay constants and the absolute ages of the primary standards adopted. Nevertheless, to allow an easy comparison between the different laboratory results, we used the constants of Steiger and Jäger (1977) and the ages listed by Renne et al. (1998) for the primary and secondary standards. We also provide a recalibrated age using the latest set of decay constants and standard ages proposed by Renne et al. (2010).

4.2.1. IGGCAS

Three aliquots, A-1, A2 (Check this with author) and A-6, were analyzed at the $^{40}Ar/^{39}Ar$ laboratory in IGGCAS, of which A-1 and A-2 were dated using the single-grain laser fusion technique and A-6 was measured by using the step-heating method.

Aliquots were wrapped in aluminum foil to form wafers. The wafer sizes 4.0 mm in diameter and 2.0 mm in thickness, and stacked in quartz vials with the standards TCs sanidine (28.34 ± 0.16 Ma, Renne et al., 1998) as neutron flux monitor. The vial was 30 mm in length with an inner diameter of 5.0 mm. Then the vials were sealed in vacuo and put in a quartz canister. The canister was wrapped with cadmium foil (0.5 mm in thickness) for shielding slow neutrons to minimize undesirable interference reactions during the irradiation. A-1, A-2 and A-6 were irradiated for 18 h, 20 h and 25 h separately to determine if there is any effect from varying the irradiation times. The irradiations were carried out in position H8 of 49-2 Nuclear Reactor (49-2 NR), Beijing (China), with a neutron flux of 6.5×10^{12} n (cm^2s^{-1}). J-values obtained for A-1, A-2 and A-6 are 0.0030980 ± 0.0000310, 0.0031810 ± 0.0000801 and 0.0035946 ± 0.0000410 respectively. The H8 position lies in the core of the reactor and receives flux from all directions. Specimens were rotated during the irradiation to receive homogeneously distributed neutrons.

Crystals of A-1 and A-2 were moved into the wells of a copper sample holder and fused grain by grain using a continuous CO_2 laser with a maximum output of 50 W. The gas fraction for each extraction was purified for 2 min using two SAES NP10 Zr–Al getters (one was set at 400 °C and the other at room temperature). The purified gas was introduced into and analyzed by a VG5400 mass spectrometer using 13 cycles of peak-hopping. Mass discrimination was monitored using an on-line air pipette from which multiple measurements were made before, during and after the experiment. The mean value over this period is 1.0060 ± 0.0002 per atomic mass unit. Blanks were monitored every 3 measurements, and were in the range from 3.0×10^{-17} to 3.5×10^{-17} mol for ^{40}Ar.

A-6 was move to a double vacuum resistance furnace and heated stepwise from 750 to 1420 °C. The released gas was purified by four SAES NP10 Zr–Al getters. The argon isotopic composition was measured using a VG5400 mass-spectrometer.

4.2.2. National Taiwan University

Grains from the aliquot A-3 were loaded into wells in an aluminum disk of 19 mm diameter and 2–3 mm thickness. FCs was used as the fluence monitor in this irradiation using 19 grains. FCs was loaded in the well between those of YBCs in the same disk. The samples were shielded with Cd and irradiated in the McMaster Nuclear Reactor in Hamilton (Ontario, Canada) for 20 h, with a neutron flux of approximately 3×10^{16} neutrons/cm^2. The J-values were calculated relative to FCs = 28.02 ± 0.16 Ma (Renne et al., 1998). The mean J-value (0.0073729 ± 0.0000578) was computed from gas composition of FCs grains irradiated in the same disk.

After irradiation, the YBCs grains were fused using a 50W US Nd-YAG laser operated in continuous mode. Ar gas was purified by two SAES NP10 Zr–Al getters (one operated at room temperature, the other one operated at 400 °C) and then measured using a VG3600 gas mass-spectrometer. Mass discrimination was monitored using an automatic air pipette, and the mean value over this period is 1.018644 ± 0.005093 per atomic mass unit. The correction factors for interfering isotopes were $(^{39}Ar/^{37}Ar)_{Ca}$ = 0.00065 ± 0.00003,

Table 1
Chemical compositions of YBC phonolite (wt.%).

Sample	SiO_2	TiO_2	Al_2O_3	MaO	MgO	CaO	Na_2O	K_2O	P_2O_5	MnO	Fe_2O_3	FeO	LOI	Total
Phonolite	54.39	0.95	15.24	0.19	0.83	4.04	4.82	7.28	0.13	0.31	6.95	1.85	2.08	99.1

Major element abundance was determined by using an X-ray fluorescence spectrometry (XRF) method. Analytical uncertainties range from 2% to 5%.

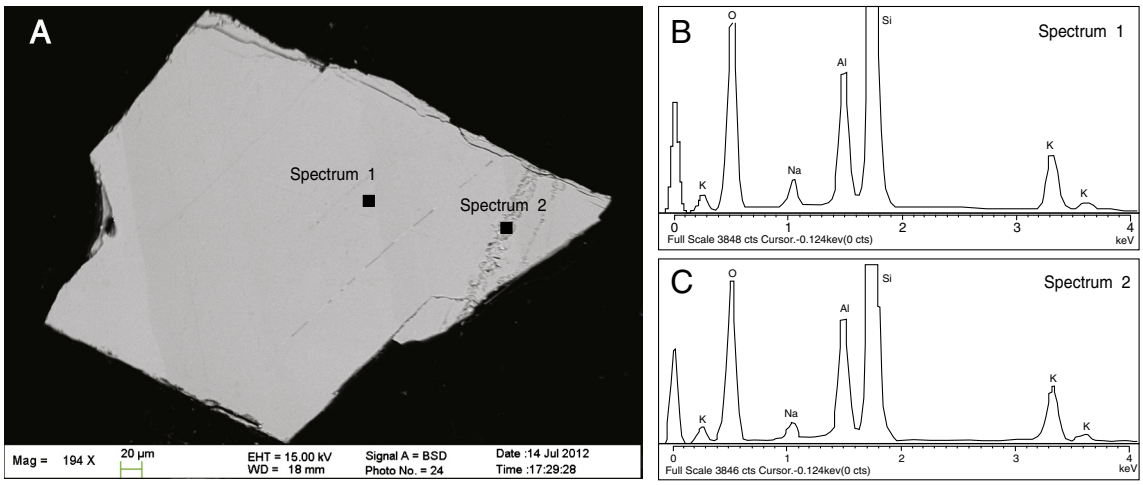

Fig. 4. Backscattered electron image of a YBC sanidine crystal (A). Regular and authigenic sanidine crystal characterizes the crystal. Scratches (right side) may be induced from sample preparations. B and C are the electron microprobe analyses on the flat and scratched areas, showing no difference in chemical composition between the two analyses. The analyses indicate that the YBCs are chemically pure K-feldspar.

$(^{36}Ar/^{37}Ar)_{Ca} = 0.000255 \pm 0.00013$ and $(^{40}Ar/^{39}Ar)_K = 0.0287 \pm 0.0014$. Ages were calculated from Ar isotopic ratios measured after corrections made for mass discrimination, interfering nuclear reactions, procedural blanks, and atmospheric Ar contamination. Blanks were monitored every 3 to 4 steps, and ^{40}Ar blanks range from 2×10^{-17} to 3×10^{-17} mol.

4.2.3. Curtin University

Crystals from aliquot A-4 were loaded into large wells of two 1.9 cm diameter and 0.3 cm depth aluminum disks; each large well was bracketed by three small holes. YBCs sanidine and HB3gr and GA1550 standards were put in the same wells whereas FCs was loaded in bracketing small holes. Two separated irradiations (A-4-1 and A-4-2) of different durations were carried out; in the first irradiation (A-4-1) YBCs was irradiated together with FCs, GA1550 and HB3gr for 2 h; in the second irradiation (A-4-2) YBCs was irradiated with GA1550 and HB3gr for 25 h. The FCs (28.02 ± 0.16 Ma), Ga1550 (98.79 ± 0.56 Ma) and HB3gr (1074 ± 5 Ma) standards were used as a neutron fluence monitor for which good inter-grain reproducibility has been demonstrated (Renne et al., 1998; Jourdan et al., 2006; Jourdan and Renne, 2007). The disks were Cd-shielded (to minimize undesirable nuclear interference reactions) and irradiated in the McMaster University nuclear reactor (Hamilton, Canada) in position 5 C.

The mean J-value was computed from standard grains, determined as the weighted mean and standard deviation of J-values for each irradiation disk. Mass discrimination was monitored using an automatic air pipette and provided mean values ranging from 1.005296 ± 0.002815 to 1.006490 ± 0.003523 per atomic mass unit. The correction factors for interfering isotopes were $(^{39}Ar/^{37}Ar)_{Ca} = 7.30 \times 10 - 4$ (±11%), $(^{36}Ar/^{37}Ar)_{Ca} = 2.82 \times 10 - 4$ (±1%) and $(^{40}Ar/^{39}Ar)_K = 6.76 \times 10 - 4$ (±32%). The $^{40}Ar/^{39}Ar$ analyses were performed at the Western Australian Argon Isotope Facility at Curtin University. The grains were fused using a 110 W continuous Nd-YAG (IR; 1064 nm) laser system. The gas was purified in a stainless steel extraction line using two SAES AP10 getters (one operated at room temperature, the other one operated at 400 °C) and a GP 50 getter operated at 400 °C. Ar isotopes were measured in static mode using a MAP 215–50 mass spectrometer using 9 to 10 cycles of peak-hopping. Blanks were monitored every 3 to 4 steps, and typical ^{40}Ar blanks range from 1×10^{-16} to 2×10^{-16} mol.

4.2.4. Gif-Sur-Yvette of CEA-CNRS UVSQ

YBC sanidine crystals were loaded in a single pit in an aluminum disk and irradiated 90 min (Irr 34) in the β1 tube of the OSIRIS reactor (CEA Saclay, France). After irradiation, crystals were transferred one by one into a copper sample holder and then loaded into a differential vacuum Cleartran© window. Ten crystals were individually fused at about 12% of the full laser power. Ar isotopes were analyzed using a VG5400 mass spectrometer equipped with a single ion counter (Balzers© SEV 217 SEN) following procedures outlined in Nomade et al. (2010). Each Ar isotope measurement consists of 20 cycles of peak switching of the argon isotopes. Neutron fluence (J) was monitored by co-irradiation of Alder Creek Sanidine (ACS-2, Nomade et al., 2005) placed in the same pit as the YBCs. The J value was determined from analyses of five single ACS-2 crystals. The corresponding J value (see online supplement full data table) was calculated using an age of 1.193 ± 0.001 Ma (Nomade et al., 2005). Procedural blanks were measured every three or four crystals depending on the sample beam size previously measured. For a typical 9-min static blank, typical backgrounds are about 2.0 to 2.2×10^{-17} and 5.0 to 6.0×10^{-19} mol for ^{40}Ar and ^{36}Ar, respectively. The precision and accuracy of the mass discrimination correction were monitored by daily measurements of air argon (see full experimental description in Nomade et al., 2010). Nucleogenic production ratios used to correct for reactor-produced Ar isotopes from K and Ca are the same as those used in Nomade et al. (2010).

4.3. Results

All raw data were processed using the ArArCALC software (Koppers, 2002) and using the total decay constant (λ) of 5.543×10^{-10} yr^{-1} (Steiger and Jäger, 1977). The internal errors (analytical error

Table 2
Arithmetic mean of the individual electron microprobe compositional analyses of YBCs sanidine (wt.%).

Element	Na_2O	SiO_2	BaO	K_2O	MgO	TiO_2	CaO	Al_2O_3	Cr_2O_3	NiO	MnO	FeO	Total	K/Ca
Content	2.43	63.95	1.73	12.25	0.01	0.07	0.13	19.40	0.05	0.02	0.01	0.48	100.2	110.5

Electron microprobe analyses were performed on a JEOL JXA-8100 electron microprobe with a WDS/EDS combined micro-analyzer. Repeated analyses of standards show a typical precision of ±1% for major and ±5% for minor elements.

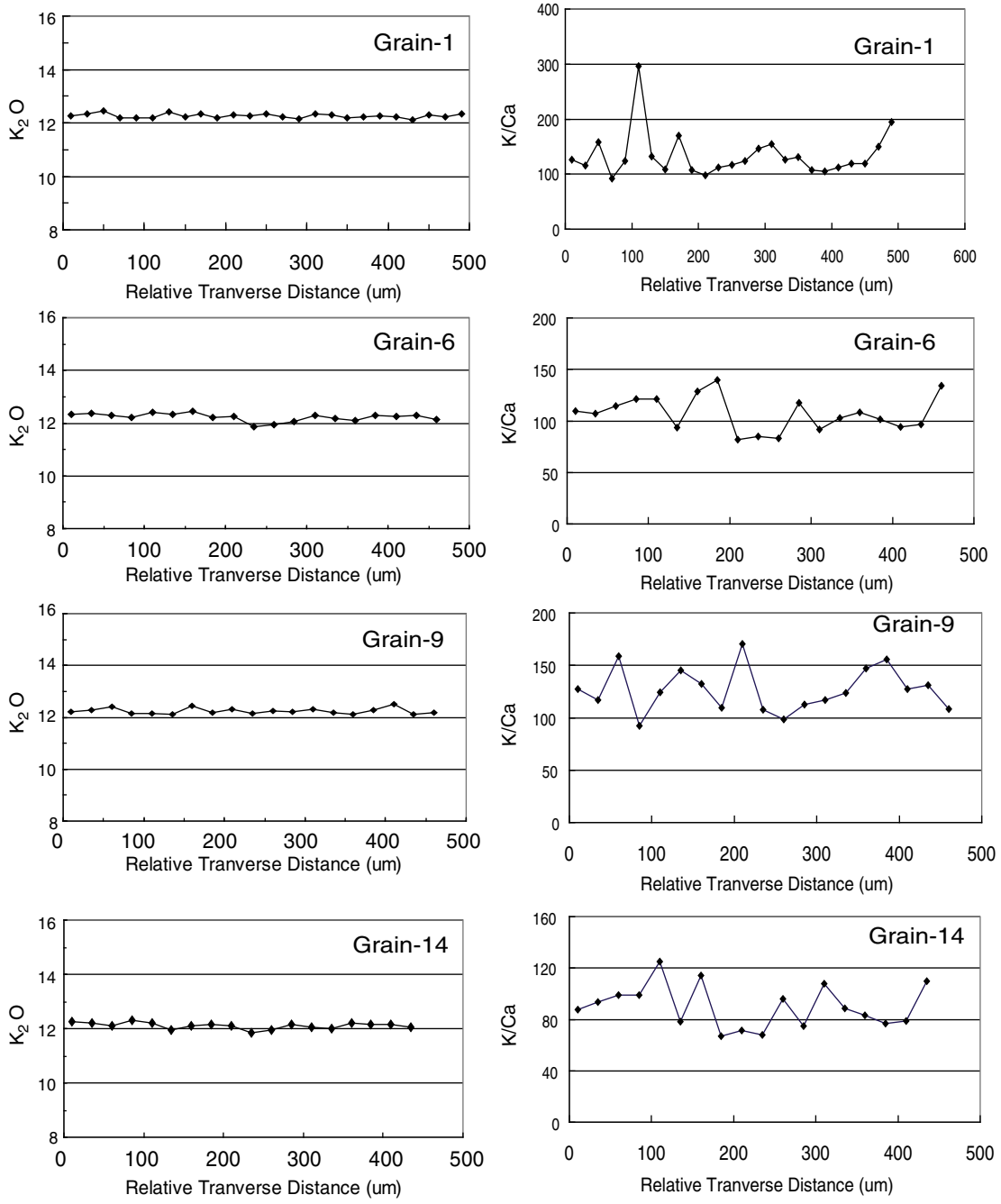

Fig. 5. Electron microprobe compositional profiles of K_2O and K/Ca (atom basis) across four selected representative grains of YBC sanidine. Grain numbers are indicated and detail data are provided in Appendix Table 1. K content is stable and K/Ca ratio varies dramatically; this is induced by the extremely low content of Ca within the YBCs.

plus error rising from blank, interaction factors, mass discrimination and J-value) are reported, to facilitate comparison of $^{40}Ar/^{39}Ar$ ages based on different standards. The errors are calculated using the following function (Koppers, 2002):

$$\sigma_T = \left[\frac{J}{\lambda(1-JF)}\right]^2 \sigma_F^2 + \left[\frac{F}{\lambda(1-JF)}\right]^2 \sigma_J^2 \quad (1)$$

where $F = {}^{40}Ar^*/{}^{39}Ar_K$, J is the J-value and λ is the total decay constant. In this error function the first term reflects the analytical error and the second term is the error on the J-value. The error in age is reported at 2σ level and in $^{40}Ar^*/^{39}Ar_K$ (F-value) at 1σ level.

The value of 295.5 ± 0.5 (Nier, 1950) is used for the atmospheric argon correction during the calculations. Although three new independent determinations of the Ar isotope composition of atmosphere are reported recently (that is, 298.56 ± 0.31 (Lee et al., 2006) and 298.709 ± 0.096 (Valkiers et al., 2010) for modern atmosphere, 143 ± 24 (Pujol et al., 2013) for Archaean atmosphere), the value of 295.5 ± 0.5 (Nier, 1950) is used for the age determination of current standards. Therefore, we use 295.5 ± 0.5 (Nier, 1950) for atmospheric argon correction in this study, which makes the comparison between YBCs and other standards easier.

4.3.1. Step-heating

To view the homogeneity of the distribution of potassium and argon within the YBCs grains, step-heating analysis was carried out on A-6 at IGGCAS. The results are presented in Appendix Table 2, and the age spectrum and inverse isochron are shown in Fig. 6.

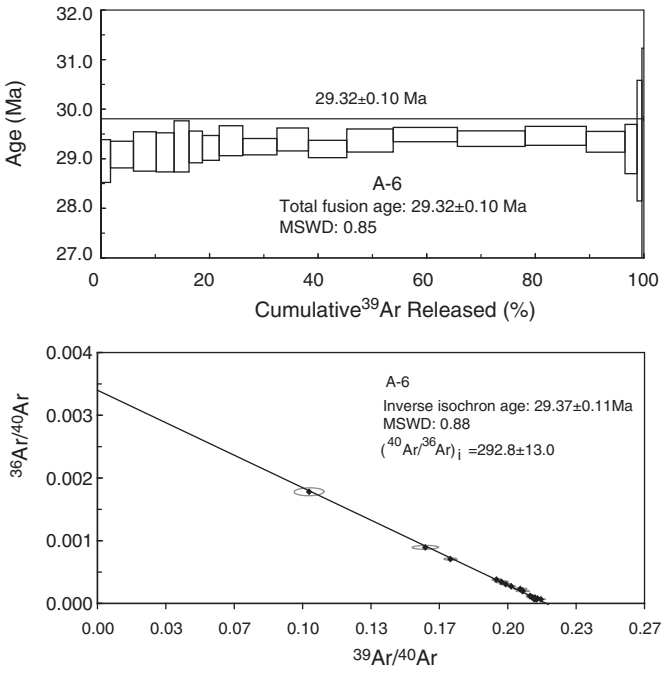

Fig. 6. Age spectra and inverse isochrons obtained from the step-heating experiments for YBCs. Detailed analytical data are given in Appendix Table 2.

A well defined plateau comprising 100% of the total $^{39}Ar_K$ released was obtained from the step-heating result, suggesting homogenous distribution of potassium and radiogenic ^{40}Ar within the YBCs crystals at the multi-grain level (Fig. 6). The obtained plateau age is 29.32 ± 0.16 Ma (MSWD, mean square weighted deviation, value 0.85), which is in good agreement with its respective inverse isochron age of 29.33 ± 0.17 Ma (MSWD value 0.88). The $^{40}Ar/^{36}Ar$ intercept in the inverse diagram, 293 ± 13, is statistically indistinguishable from the atmospheric value adopted during the analysis (295.5 ± 0.5), suggesting that there is no detectable excess argon within the YBCs grains. The K/Ca ratios are in a wide range from 14 to 98 (Appendix Table 2), suggesting that it is not a reliable indicator as expected from such a Ca-poor mineral (e.g., Baksi et al., 1996; Phillips and Matchan, 2013). Petrologically, sanidine bears very low calcium (Phillips and Matchan, 2013), resulting in low ^{37}Ar production during irradiation. This causes $^{39}Ar/^{37}Ar$ measurement inaccurate, and therefore results in a wide range of K/Ca values. Usually, K/Ca ratio of a sanidine is not a useful index.

4.3.2. Single grain total fusion

Results of single grain total fusion are given in Appendix Table 3, and the probability diagrams are shown in Fig. 7. The mean $^{40}Ar^*/^{39}Ar_K$ ratios, ages, errors and MSWDs for the analyses on different aliquots are summarized in Table 3.

Sixty grains from A-1 were fused, each of them yielding virtually identical ages relative to TCs and ranging from 29.12 ± 0.26 to 29.53 ± 0.33 Ma (Appendix Table 3, Fig. 7). The age population forms a well-defined Gaussian distribution (Fig. 7). The weighted mean age is 29.31 ± 0.07 Ma at the 95% confidence level, with an MSWD value of 0.74 and probability of 0.93 (Fig. 7, Table 3).

Fourteen single-grain ages from the A-3 aliquot in the range 28.97 ± 0.39 to 29.55 ± 0.49 Ma (Appendix Table 3) relative to FCs, and also give a well-defined normal distribution (Fig. 7), yielding a mean age of 29.32 ± 0.24 Ma at the 95% confidence level with an MSWD value of 0.76 and probability of 0.71 (Fig. 7, Table 3).

The single-grain ages obtained from ten grains of A-5 range from 29.06 ± 0.08 to 29.37 ± 0.07 Ma relative to ACs (Appendix Table 3, Fig. 7) in a normal distribution with a mean value of 29.25 ± 0.08 Ma at the 95% confidence level, with an MSWD value of 1.09 and probability of 0.37 (Fig. 7, Table 3).

Thirteen grains from the A-4-1 aliquot (2 h irradiation) gave ages ranging from 29.25 ± 0.41 to 29.68 ± 0.33 Ma against GA1550 (Fig. 7, A-4-1-GA), from 29.06 ± 0.40 to 29.50 ± 0.33 Ma against FCs (Fig. 7, A-4-1-FC) and from 29.59 ± 0.41 to 30.03 ± 0.34 Ma against HB3gr (Fig. 7, A-4-1-HB) (Appendix Table 3). They yielded weighted mean ages of 29.46 ± 0.16 Ma (against GA1550), 29.27 ± 0.36 Ma (against FCs) and 29.80 ± 0.42 Ma (against HB3gr) respectively (Table 3 and Fig. 7). Twelve grains from the A-4-2 batch (25 h irradiation) yielded single-grain ages in the ranges of 29.17 ± 0.35–29.96 ± 1.49 Ma against GA1550 (Fig. 7, A-4-2-GA, Appendix Table 3) and ranging between 28.85 ± 0.70 and 29.87 ± 1.48 against HB3gr (Fig. 7, A-4-2-HB, Appendix Table 3). They yielded weighted mean ages of 29.24 ± 0.15 Ma when against GA1550 and 29.16 ± 0.17 Ma when against HB3gr (Table 3, Fig. 7). The MSWDs of these means range from 0.28 to 0.51 and probability form 0.91 to 0.99. (Table 3).

4.4. Discussion

4.4.1. Homogeneity and reproducibility

The YBC sanidine grains display homogeneous K_2O distribution as shown by the electron microprobe analyses (Fig. 2). The step-heating experiment yielded a well defined plateau that includes 100% of released ^{39}Ar (Fig. 6), suggesting homogeneous $^{40}Ar^*$ and K within the YBCs grains at the multi-grain level. The consistency of the total-gas age, plateau age and inverse-isochron age (Fig. 6, Appendix Table 3) demonstrates that excess argon and alteration effects are not apparent in YBCs crystals.

The five F-value ($^{40}Ar^*/^{39}Ar_K$) suites of single-grain-laser-fusion obtained from the five irradiations vary in small ranges respectively: 5.2379 ± 0.0339–5.3142 ± 0.0302 (A-1), 2.1905 ± 0.0109–2.2342 ± 0.0111 (A-3), 1.6819 ± 0.0205–1.7098 ± 0.0101 (A-4-1), 21.9025 ± 0.1531–22.2322 ± 0.1254 (A-4-2) and 22.9193 ± 0.0641–23.1597 ± 0.0567 (A-5).

In the probability plots, all of the F-values of each suite, apart from one point in A-4-2 (Fig. 8), scatter about a straight line of slope around 1 (Fig. 8), suggesting that the data are from a single Gaussian population. The weighted mean F-values (Table 3, Fig. 8) for the six suites are 5.2741 ± 0.0111 (A-1, MSWD = 0.74, N = 60), 2.2197 ± 0.0085 (A-3, MSWD = 1.19, N = 14), 1.6996 ± 0.0040 (A-4-1, MSWD = 0.28, N = 12), 22.0430 ± 0.0600 (A-4-2, MSWD = 0.51, N = 13) and 23.0790 ± 0.0640 (A-5, MSWD = 1.09, N = 10), respectively. The six standard deviation values of the mean F-values describe the overall dispersion of the data and range from 0.29% to 0.83%, or 0.29% to 0.53% when an outlier datum in A-4-2 is rejected (Table 3).

The results above show that the YBCs crystals are homogenous at the single-crystal level and have strong reproducibility between analyses.

The averaged radiogenic $^{40}Ar^*$ accounts for 97.1–99.3% of the total argon within the YBCs crystals, suggesting that the atmospheric argon within the crystal is a very small portion (2.9–0.7%) (Table 3).

4.4.2. The calibrated age of YBCs

The apparent individual ages shown in Section 4.3.2 are individually obtained against different standards of TCs (for A-1), FCs (for A-3 and A-4-1), ACs (for A-5), Ga1550 (for A-4-1 and A-4-2) and HB3gr (for A-4-1 and A-4-2). These ages are not directly comparable unless they are intercalibrated to the same standard.

The ages of TCs, FCs, ACs, Ga1550 and HB3gr have been intercalibrated repeatedly (such as Baksi et al., 1996; Renne et al., 1998, 2010; McDougall and Harrison, 1999; Spell and McDougall, 2003; Daze' et al., 2003; Jourdan et al., 2006; Jourdan and Renne, 2007; Kuiper et al., 2008; Phillips and Matchan, 2013). In this study, we use secondary standard ages of 28.34 ± 0.16 Ma for TCs, 28.02 ± 0.16 Ma for FCs, 1.194 ± 0.007 Ma for ACs, and 98.79 ± 0.56 Ma calibrated against the primary standard GA1550 from Renne et al. (1998).

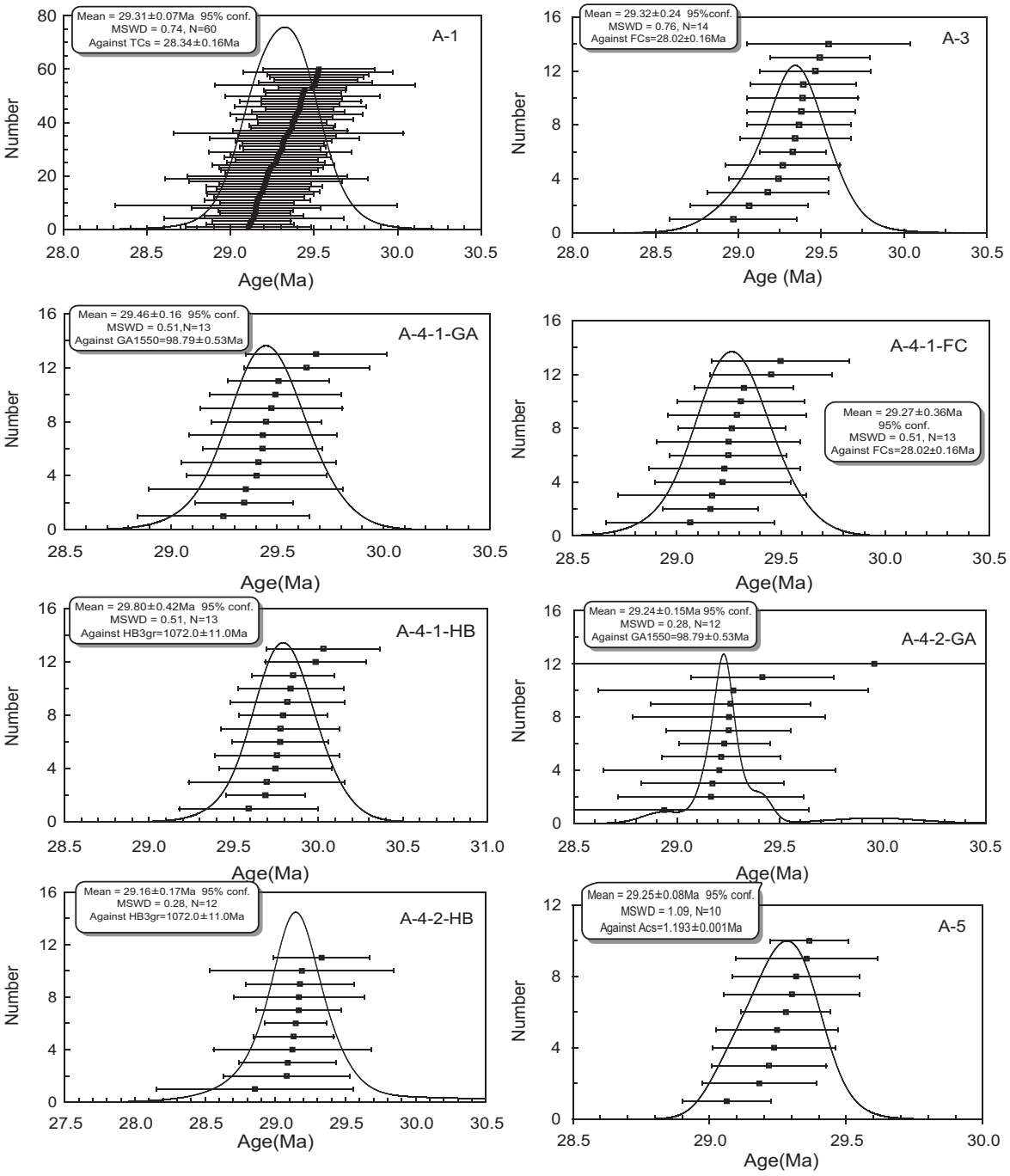

Fig. 7. The probability plots of single-grain laser-fusion results for different aliquots of YBCs. The mean ages, MSWD values, and standards are shown. The errors are 1 σ. Detailed analytical data are given by Appendix Table 2.

The age of 1074 ± 5 Ma for HB3gr, calibrated relative to FCs with age of 28.02 ± 0.16 Ma given by Jourdan et al. (2006) and Jourdan and Renne (2007), is adopted in age calculation in the present study.

We therefore recalculate the original single-grain ages as 29.31 ± 0.07 (A-1, against TCs), 29.32 ± 0.24 Ma (A-3, against FCs), 29.46 ± 0.16 Ma (A-4-1-GA, against GA1550), 29.27 ± 0.36 Ma (A-4-1-FC, against FCs), 29.80 ± 0.42 Ma (A-4-1-HB, against HB3gr), 29.24 ± 0.15 Ma (A-4-2-GA, against GA1550), 29.16 ± 0.17 Ma (A-4-2-HB, against HB3gr) and 29.28 ± 0.08 Ma for A-5 (against ACs).

Fig. 9B shows that all but one apparent ages are consistent at the 2σ level. HB3gr from the 2 h irradiation yielded an age for YBCs of 29.80 ± 0.42 Ma, that is significantly older and less precise than given against other standards. This apparent discrepancy is likely due to the fact that HB3gr, which is a 1074 Ma old standard, has been significantly under-irradiated during a short (2 h) irradiation. The F-value of HB3gr is 1074[1] (e.g. compared to an F-value of 21 for FCs for 2 h irradiation), largely too high to allow accurate $^{40}Ar/^{39}Ar$ measurements (McDougal and Harrison, 1999). Therefore, due to the potential inaccuracy of this measurement, we choose not to include this data set in the final R-value and age calculation. In the probability plot (Fig. 9A), all the other weighted mean ages scatter along a straight line of slope close to 1, suggesting that these data are from the same normal distribution.

[1] This ratio is not to be mistaken with an age of 1074 Ma. These two numbers are equal only as a coincidence.

Table 3
Summary of $^{40}Ar^{*}/^{39}Ar_{K}$ (F-value) results for YBCs.

Aliquot	N	Standard	Irradiation reactor	Irradiation duration (h)	F-value ($^{40}Ar^{*}/^{39}Ar_{K}$) ±2σ (±%)	Standard deviation (1σ) (%)	MSWD	$^{40}Ar^{*}$ (%)
A-1	60	TCs	49-2, H8 (Beijing, China)	18	5.2741 ±0.0111 (±0.21%)	0.0226 (0.43%)	0.74	98.1
A-3	14	FCs	McMaster, 5C (Hamilton, Canada)	20	2.2197 ±0.0085 (±0.38%)	0.0117 (0.53%)	1.19	93.1
A-4-1	13	FCs GA1550 HB3gr	McMaster, 5C (Hamilton, Canada)	2	22.0431 ±0.0600 (±0.27%)	0.0638 (0.35%)	0.51	97.9
A-4-2	12	GA1550 HB3gr	McMaster, 5C (Hamilton, Canada)	25	1.6996 ±0.0040 (±0.24%)	0.0063 (0.38%)	0.28	97.1
A-5	10	ACs	OSIRIS, β1 (CEA Saclay, France)	1.5	23.0790 ±0.0640 (±0.28%)	0.067846 (0.29%)	1.09	99.3

F-values were calculated using the weighted-mean and error of the weighted-mean. Irradiation duration, standard deviation (1σ) and MSWD are indicated. N denotes the number of the grains analyzed.

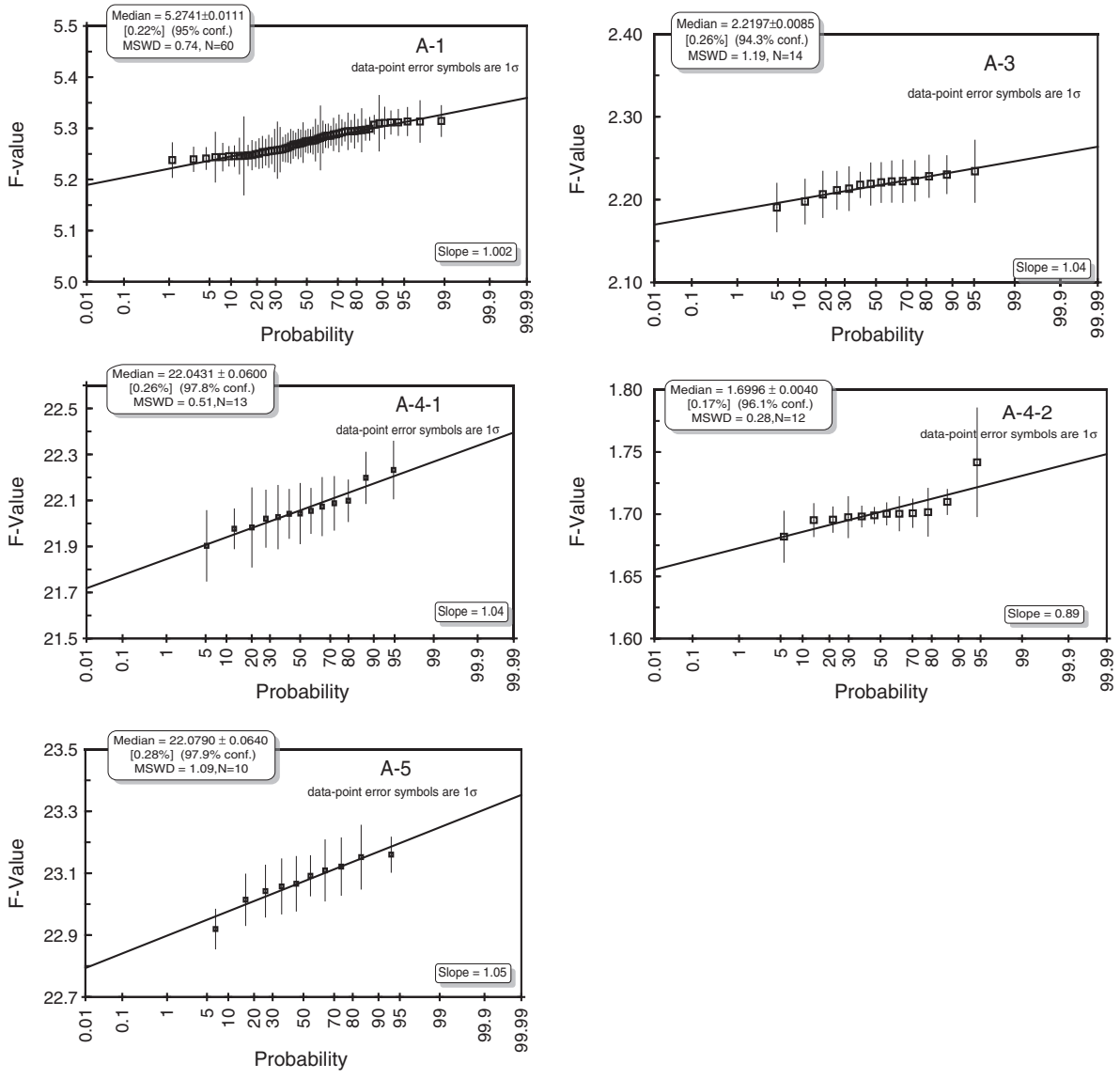

Fig. 8. Probability plots of $^{40}Ar^{*}/^{39}Ar_{K}$ ratios (F-value) of six aliquots of YBCs. Apart from A-4-2, all the suite of F-values form a line with slope around 1, suggesting that they come from a single normal distribution. One point on the suite of A-4-2 values is anomalous, implying that it is an outlier and should be rejected in the calculations.

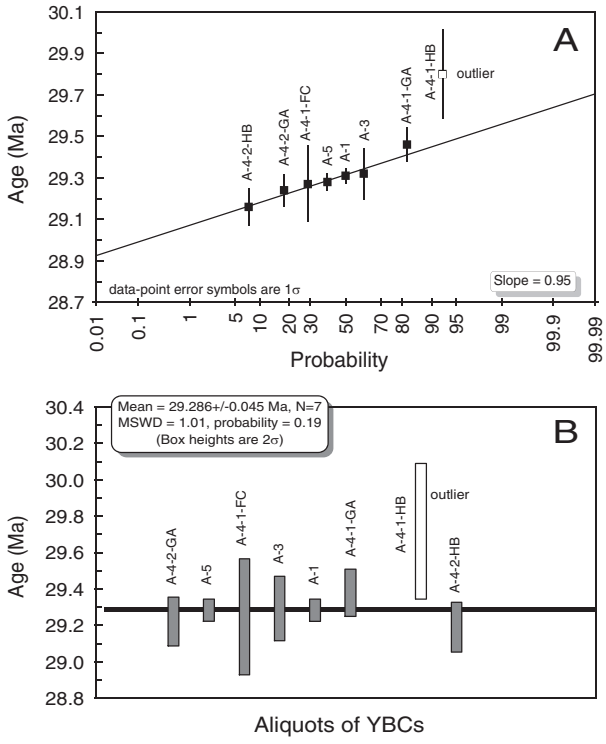

Fig. 9. Probability plot of weighted mean ages and calibration of YBCs age. Apart from one point (outlier), the other eight weighted mean ages distribute around a line of slope = 0.95, implying they are from the same Gaussian distribution (A). The mean value of these eight ages is taken as the finally-calibrated age for YBCs (B), when one outlier is rejected. The MSWD of the mean is close to 1, suggesting that the mean age properly reflects the analytical error.

All the weighted mean age standard deviations (1σ) are in the range 0.42% to 0.52% and define a homogenous age population as shown by an MSWD value of 1.1 and P-value of 0.35. This is even more remarkable because these ages come from different duration of irradiation, neutron flux, standard usage, mass-spectrometers and laboratory protocols.

The intercalibrated age for YBCs is given as the weighted mean of seven ages obtained for the different aliquot of YBCs (Fig. 7) and is shown in Fig. 9B. When calculated relatively to the ^{40}K decay constants of Steiger and Jager (1977) the age of YBCs is 29.286 ± 0.045 Ma (external error ±0.206) Ma and is given a 2σ level. Its relative standard deviation is 0.28%, and MSWD value of 1.11. This age corresponds to a mean $^{40}Ar^*/^{40}K$ value of $(1.716 \pm 0.003) \times 10^{-3}$, which is independent of the values of the decay constants used for calculation. When using the decay constants of Steiger and Jäger (1977), the external error was calculated by using the following error propagation functions:

$$y = f(x_1, x_2, \ldots, x_n) \tag{2}$$

$$\Delta_y = \left|\frac{\partial f}{\partial x_1}\right|\Delta_{x_1} + \left|\frac{\partial f}{\partial x_2}\right|\Delta_{x_2} + \cdots + \left|\frac{\partial f}{\partial x_n}\right|\Delta_{x_n} \tag{3}$$

More recently, Renne et al. (2010) proposed a revised value of the ^{40}K decay constants, branching ratio, and associated standard ages based on an extensive calibration between $^{40}Ar/^{39}Ar$ and $^{238}U/^{206}Pb$ ages. Using the $^{40}Ar^*/^{40}K$ value calculated above and the constant proposed by Renne et al. (2010) yields a YBCs age of 29.584 ± 0.045 Ma (2σ). Including all sources of errors and following the Monte Carlo optimization calculation of Renne et al. (2010) that takes into account correlated errors, an external uncertainty of ±0.067 Ma is obtained.

4.4.3. Intercalibration factors (R_X^Y-values)

Analyses of A-4-1, A-4-2 and A-5 using disks allow a good constraint on the F-values of the standards and YBCs and permit us to calculate the R-values of YBCs relative to the reference standards. The intercalibration factors (R_X^Y-values) allow a direct comparison between standards Y and X. This calculation was initially proposed by Renne et al. (1998) and then widely used in standard calibration works (e.g., Renne et al., 1998; Daze' et al., 2003; Jourdan et al., 2006; Jourdan and Renne, 2007; Phillips and Matchan, 2013). R_X^Y can be determined from reported ages using the following equations proposed by Renne et al. (1998):

$$R_X^Y = \frac{F_Y}{F_X} \tag{4}$$

where F is the F-value ($^{40}Ar^*/^{39}Ar_K$) (Table 4), Y and X denote the standards.

The calculated R_X^{YBCs} values are (Table 4): $R_{FCs}^{YBCs} = 1.044296 \pm 0.003968$, $R_{GA1550}^{YBCs} = 0.291261 \pm 0.001148$ $R_{ACs}^{YBCs} = 24.443066 \pm 0.068432$, and $R_{HB3gr}^{YBCs} = 0.020312 \pm 0.000885$. The uncertainty of each R-value is calculated following a standard error propagation calculation using the uncertainties associated with the two F-values. In the future, ages determined using the YBCs standards can be therefore compared with any these standards by using these R_X^Y values or alternatively, the age of YBCs can be recalculated if the age associated with any of these standards changes.

This study provides a complete multi-laboratory intercalibration study of the YBC sanidine, against the most robust set of $^{40}Ar/^{39}Ar$ standards widely adopted by the community. We have shown that YBCs is homogenous both in term of composition and age distributions and thus, is deemed suitable as a new $^{40}Ar/^{39}Ar$ standard to be used.

In the future, in particular considering the improvement of multi-collection noble-gas mass spectrometers, ultra-high precision results will be obtained and reproducibility will be defined more precisely. In particular, we will test the homogeneity of the $^{40}Ar/^{39}Ar$ distribution of the sanidine via step-heating, in comparison to the work of Phillips and Matchan (2013) on the FC sanidine standard. More aliquots of YBCs have been distributed to several laboratories for comparative analysis. An additional, larger quantity of this sanidine standard has been prepared for wider distribution for routine analysis.

5. Conclusions

We successfully evaluate, date and intercalibrate a new sanidine standard, YBCs, for $^{40}Ar/^{39}Ar$ dating. The YBCs sanidine samples are from a phonolite from the Tibetan plateau with high alkali content. Electronic microprobe analyses show that the K content is high (12.21 ± 0.04 wt.%) and chemically homogeneous across the crystals.

Aliquots of YBCs were distributed to four international laboratories for $^{40}Ar/^{39}Ar$ analyses. Step-heating result shows a well defined plateau accounting for 100% of the released ^{39}Ar showing homogenous distributions of $^{40}Ar^*$ and K within the crystals. The concordance of total gas age, plateau age and inverse isochron age suggests that there are no effects from alteration and excess argon. Single grain laser-fusion results from the four laboratories show that the YBCs crystals are homogenous in $^{40}Ar^*/^{39}Ar_K$ at the single crystal level and have strong between-analysis reproducibility with an overall dispersion range from 0.29% to 0.53%. The weighted mean ages from different irradiations and against different standards vary within a small range of 0.3 Ma (±0.51%) suggesting a strong reproducibility of age; variations are not related to the duration of irradiation, neutron flux, and standard usage. These observations indicate that the YBCs sanidine is suitable as a single-grain $^{40}Ar/^{39}Ar$ dating standard. The calibrated age of YBCs is 29.286 ± 0.045 Ma (ext. ±0.206) Ma; this age is 29.584 ± 0.045 Ma (ext. ±0.067) when the more recent decay constant ($\lambda = (5.5492 \pm 0.0054) \times 10^{-10} a^{-1}$) proposed by Renne et al. (2010). Finally, the

Table 4
R-values of YBCs relative to FCs, GA1550, HB3gr and ACs.

Irradiation	Aliquot	F_{std}	$\pm\sigma(F_{std})$	F_{YBCs}	$\pm\sigma(F_{YBCs})$	$R_{YBCs/std}$	$\pm\sigma(R)$
GA1550/YBCs							
16t2h	A-4-1	75.4277	0.3664	22.0431	0.0638	0.292240	0.001223
16t25h	A-4-2	5.8542	0.0191	1.6996	0.0064	0.290321	0.001072
Weighted mean of $R_{YBCs/GA1550}$ (±error of the weighted mean) 0.291261 ± 0.001148							
HB3gr/YBCs							
16t2h	A-4-1	1074.38	15.43	22.0431	0.0638	0.020517	0.000082
16t25h	A-4-2	84.867	0.381	1.6996	0.0064	0.020027	0.000104
Weighted mean of $R_{YBCs/HB3gr}$ (±error of the weighted mean) 0.020312 ± 0.000885							
FCs/YBCs							
16t2h	A-4-1	21.1081	0.2585	1.6996	0.0064	1.044296	0.003968
ACs/YBCs							
Irr-34	A-5	0.9439	0.0072	23.0718	0.0514	24.443066	0.068432

intercalibration factors (R^{Y}_{X}-values) of YBCs relative to the other five currently used standards were calculated.

Supplementary data to this article can be found online at http://dx.doi.org/10.1016/j.chemgeo.2014.09.003.

Acknowledgments

We are very grateful to the anonymous reviewers for their thorough and helpful reviews and constructive suggestions. Comments by Donald Dingwell, the Editor of Chemical Geology is very gratefully acknowledged. This study was jointly funded by the China Natural Science Foundation (41025010, 41221002) and the "Strategic Priority Research Program" of the Chinese Academy of Sciences (XDB03020203), and the "Innovation Project" of IGGCAS.

References

Baksi, A.K., Archibald, D.A., Farrar, E., 1996. Intercalibration of $^{40}Ar/^{39}Ar$ dating standards. Chem. Geol. 129, 307–324.
Chung, S.-L., Chu, M.-F., Zhang, Y., Xie, Y., Lo, C.-H., Lee, T.-Y., Lan, C.-Y., Li, X., Zhang, Q., Wang, Y., 2005. Tibetan tectonic evolution inferred from spatial and temporal variations in post-collisional magmatism. Earth Sci. Rev. 68 (3–4), 173–196.
Daze', A., Lee, J.K.W., Villeneuve, M., 2003. An intercalibration study of the Fish Canyon sanidine and biotite $^{40}Ar/^{39}Ar$ standards and some comments on the age of the Fish Canyon Tuff. Chem. Geol. 199, 111–127.
Ding, L., Zhou, Y., Zhang, J., Deng, W., 2000. Geologic relationships and geochronology of the Cenozoic volcanoes and interbedded weathered mantles of Yulinshan in Qiangtang, North Tibet. Chin. Sci. Bull. 45, 2214–2220.
Ding, L., Kapp, P., Yue, Y., Lai, Q., 2007. Postcollisional calc-alkaline lavas and xenoliths from the southern Qiangtang terrane, central Tibet. Earth Planet. Sci. Lett. 254 (1–2), 28–38.
Heri, A.R., Robyr, M., Villa, I.M., 2014. Petrology and geochronology of 'muscovite age standard' B4M. In: Jourdan, F., Mark, D.F., Verati, C. (Eds.), Advances in $^{40}Ar/^{39}Ar$ Dating: from Archaeology to Planetary Sciences Geological Society 378. Special Publications, London, pp. 69–789.
Jiang, Y.-H., Jiang, S.-Y., Ling, H.-F., Dai, B.-Z., 2006. Low-degree melting of a metasomatized lithospheric mantle for the origin of Cenozoic Yulong monzogranite- porphyry, east Tibet: geochemical and Sr–Nd–Pb–Hf isotopic constraints. Earth Planet. Sci. Lett. 241 (3–4), 617–633.
Jourdan, F., Renne, P.R., 2007. Age calibration of the Fish Canyon sanidine $^{40}Ar/^{39}Ar$ dating standard using primary K–Ar standards. Geochim. Cosmochim. Acta 71, 387–402.
Jourdan, F., Verati, C., Féraud, G., 2006. Intercalibration of the Hb3gr $^{40}Ar/^{39}Ar$ dating standard. Chem. Geol. 231, 177–189.
Koppers, A.A.P., 2002. ArArCALC—software for $^{40}Ar/^{39}Ar$ age calculations. Comput. Geosci. 28, 605–619.
Kuiper, K.F., Deino, A., Hilgen, F.J., Krijgsman, W., Renne, P.R., Wijbrans, J.R., 2008. Synchronizing rock clocks of Earth history. Science 320, 500–504.
Lee, J.Y., Marti, K., Severinghaus, K., Kawamura, K., Yoo, H.S., Lee, J.B., Kim, J.S., 2006. A redetermination of the isotopic abundances of atmospheric Ar. Geochim. Cosmochim. Acta 70, 4507–4512.
McDougall, I., Harrison, T.M., 1999. Geochronology and Thermochronology by the $^{40}Ar/^{39}Ar$ Method. Oxford Univ. Press, New York, pp. 199–204.
Nier, A.O., 1950. A redetermination of the relative abundances of the isotopes of carbon, nitrogen, oxygen, argon and potassium. Phys. Rev. 77, 789–793.
Nomade, S., Renne, P.R., Vogel, N., Deino, A.L., Sharp, W.D., Becker, T.A., Jaouni, A.R., Mundil, R., 2005. Alder Creek sanidine (ACs-2): a Quaternary $^{40}Ar/^{39}Ar$ dating standard tied to the Cobb Mountain geomagnetic event. Chem. Geol. 218, 315–338.
Nomade, S., Gauthier, A., Guillou, H., Pastre, J.F., 2010. $^{40}Ar/^{39}Ar$ temporal framework for the Alleret maar lacustrine sequence (French Massif-Central): volcanological and paleoclimatic implications. Quat. Geochronol. 5, 20–27.
Phillips, D., Matchan, E.L., 2013. Ultra-high precision $^{40}Ar/^{39}Ar$ ages for Fish Canyon Tuff and Alder Creek Rhyolite sanidine: new dating standards required? Geochim. Cosmochim. Acta 121, 229–239.
Pujol, M., Marty, B., Burgess, R., Turner, G., Philippot, P., 2013. Argon isotopic composition of Archaean atmosphere probes early Earth geodynamics. Nature 498, 87–90.
Renne, P.R., Swisher, C.C., Deino, A.L., Karner, D.B., Owens, T.L., DePaolo, D.J., 1998. Intercalibration of standards, absolute ages and uncertainties in $^{40}Ar/^{39}Ar$ dating. Chem. Geol. 145, 117–152.
Renne, R.P., Mundil, R., Balco, G., Min, K., Ludwig, K.R., 2010. Joint determination of 40 K decay constants and $^{40}Ar^{*}/^{40}K$ for the Fish Canyon sanidine standard, and improved accuracy for $^{40}Ar/^{39}Ar$ geochronology. Geochim. Cosmochim. Acta 74, 5349–5367.
Spell, T.L., McDougall, I., 2003. Characterization and calibration of $^{40}Ar/^{39}Ar$ dating standards. Chem. Geol. 198, 189–211.
Spurlin, M.S., Yin, A., Horton, B.K., Zhou, J., Wang, J., 2005. Structural evolution of the Yushu–Nangqian region and its relationship to syncollisional igneous activity, eastcentral Tibet. Geol. Soc. Am. Bull. 117 (9–10), 1293–1317.
Steiger, R.H., Jäger, E., 1977. Subcommission on geochronology: convention on the use of decay constants in geo-and cosmochronology. Earth Planet. Sci. Lett. 36, 359–362.
Valkiers, S., Vendelbo, D., Berglund, M., de Podesta, M., 2010. Preparation of argon primary measurement standards for the calibration of ion current ratios measured in argon. Int. J. Mass Spectrom. 291, 41–47.
Wang, Q., Wyman, D.A., Li, Z., Sun, W., Chung, S., Zhang, Q., Dong, H., Yu, Y., Pearson, N., Qiu, H., Zhu, T., Feng, X., 2010. Eocene north-south trending dikes in central Tibet: new constraints on the timing of east-west extension with implications for early plateau uplift? Earth Planet. Sci. Lett. 298, 205–216.
Yin, A., Harrison, T.M., 2000. Geologic evolution of the Himalayan–Tibetan orogen. Ann. Rev. Earth Planet. Sci. 28, 211–280.